Genes & Diseases

FULL LENGTH ARTICLE

Intranuclear cardiac troponin I plays a functional role in regulating *Atp2a2* expression in cardiomyocytes

Qian Lu [a,b,d,1], Bo Pan [a,b,1], Haobo Bai [c], Weian Zhao [a,b], Lingjuan Liu [a,b], Gu Li [a,b], Ruimin Liu [a,b], Tiewei Lv [a,b], Xupei Huang [d], Xi Li [e,**], Jie Tian [a,b,*]

[a] *Department of Pediatric Cardiology, Ministry of Education Key Laboratory of Child Development and Disorders, National Clinical Research Center for Child Health and Disorders, China International Science and Technology Cooperation Base of Child Development and Critical Disorders, Children's Hospital of Chongqing Medical University, Chongqing 400014, PR China*
[b] *Chongqing Key Laboratory of Pediatrics, Chongqing 400014, PR China*
[c] *Department of Orthopedic, The First Affiliated Hospital of Chongqing Medical University, Chongqing 400016, PR China*
[d] *Department of Biomedical Science, Charlie E. Schmidt College of Medicine, Florida Atlantic University, Boca Raton, FL 33431, USA*
[e] *Biology Science Institutes of Chongqing Medical University, Chongqing 400016, PR China*

Abstract In the past studies, it is shown that cardiac troponin I (cTnI, encoded by *TNNI3*), as a cytoplasmic protein, is an inhibitory subunit in troponin complex, and involves in cardiomyocyte diastolic regulation. Here, we assessed a novel role of cTnI as a nucleoprotein. Firstly, the nuclear translocation of cTnI was found in mouse, human fetuses and rat heart tissues. In addition, there were differences in percentage of intranuclear cTnI in different conditions. Based on weighted gene co-expression network analyses (WGCNA) and verification in cell experiments, a strong expression correlation was found between *TNNI3* and *Atp2a2*, which encodes sarco-endoplasmic reticulum Ca^{2+} ATPase isoform 2a (SERCA2a), and involves in ATP hydrolysis and Ca^{2+} transient. TNNI3 gain and loss caused Atpa2a2 increase/decrease in a dose-dependent manner both in mRNA and protein levels, *in vivo* and *in vitro*. By using ChIP-

* Corresponding author. Department of Cardiology, The Children's Hospital of Chongqing Medical University, 136 Zhongshan Er Road, Yu Zhong District, Chongqing 400014, PR China. Fax: +86 023 68485111.
** Corresponding author. Department of Life Science, Chongqing Medical University, 1 Yi Xue Yuan Road, Yu Zhong District, Chongqing 400016, PR China.
E-mail addresses: lixi@cqmu.edu.cn (X. Li), jietian@cqmu.edu.cn (J. Tian).
Peer review under responsibility of Chongqing Medical University.
[1] Authors contributed equally to this manuscript and shared the first authorship.

sequence we demonstrated specific binding DNA sequences of cTnI were enriched in *ATP2a2* promoter $-239 \sim -889$ region and the specific binding sequence motif of cTnI was analyzed by software as "CCAT", which has been reported to be required for *YY1* binding to the promoter region of *YY1*-related genes. Moreover, it was further verified that pcDNA3.1 (−)-TNNI3 could express cTnI proteins and increase the promoter activity of *Atp2a2* through luciferase report assay. In the end, we evaluated beat frequencies, total ATP contents, Ca^{2+} transients in *TNNI3*-siRNA myocardial cells. These findings indicated, for the first time, cTnI may regulate *Atp2a2* in cardiomyocytes as a co-regulatory factor and participate in the regulation of intracellular Ca ions.

Introduction

cTnI is an inhibitory subunit in troponin complex that binds to actin-tropomyosin and regulates muscle contraction and actin-activated myosin (actomyosin) ATPase activities.[1] cTnI has received considerable attention as a serum biomarker of myocardial tissue damages and as a key phosphoprotein that regulates cardiac function.[2,3] In recent years, linkage studies and animal experiments have confirmed that cTnI deficiency and point mutations in *TNNI3* (encodes cTnI) are linked to diastolic dysfunction and inherited cardiomyopathies.[4-9] These cardiomyopathies (CMs) show different pathological phenotypes. However, it is worth noting that all these CMs are induced by single site mutations of *TNNI3*.[7,8,10] Obviously, mutations of *TNNI3* are the initial triggers of these CMs. Moreover, cTnI loss shows strong correlation both with heart failure and aging hearts.[10-13] Although multiple factors are associated with different cardiac pathological processes, those mechanisms still cannot perfectly account for the energy metabolism disorder[14] and imbalance of Ca^{2+} regulation[6] in these cardiovascular diseases. In those *TNNI3* mutation caused cardiomyopathies, we speculate that cTnI might not just function as an inhibitory subunit in troponin complex, it may play some regulation role in the heart.

In recent years, data of some studies have indicated that cTnI do exist in nucleus.[15-17] Sahota VK et al[15] have found that TnI might regulate chromosomal stability and cell polarity in drosophila cells. Meanwhile, nuclear localization signal of cTnI has also been observed in cardiac differentiation of rat mesenchymal stem cells[16] and in myocytes that are different from human embryonic stem cells.[17] However, the mechanism of cTnI transportation into the nucleus and the function of intranuclear cTnI are largely unknown. In our previous study we have detected proteins that may potentially bind with cTnI in cardiomyocytes[18] by using Co-Immunoprecipation-Mass-Spectrum method. Surprisingly, besides some familiar cytoplasm proteins, such as cTnC (cardiac troponin C) and cTnT (cardiac troponin T), we found some nucleoproteins that might bind with cTnI, for example, histone deacetylase 1 (HDAC1).[18] As is known as another subunit of troponin, cTnT is also considered as a structural and cytoplasmic protein. It is interesting to find that, in recent findings, TnT3 shuttles to the nucleus, where it appears to perform nonclassical transcription regulatory functions.[19,20] Furthermore, Haodi Wu et al[21] have revealed that nuclear localization of mutated TNNT2 (which encodes cardiac troponin T) might contribute to epigenetic modification in pathology process of DCM (dilated cardiomyopathy). Through these evidences, it could be indicated that cTnI might play some crucial roles in the heart as a nucleoprotein.

In this study, we separated cardiac protein into nucleoprotein (Nu) and cytoplasm protein (Cy) to observe the nuclear translocation of cTnI/TnI in mice, rats and human fetus hearts. We further explored the relationship between the change of the subcellular distribution of cTnI, cardiac function in physiological and pathological conditions. By using bioinformatics analysis, *ATP2a2* was predicted to be the suspicious downstream gene of cTnI. Regulatory role of cTnI on *ATP2a2* expression was evaluated by up-regulating and knocking down TNNI3 both *in vitro* and *in vivo* experiments. We then explored the molecular mechanism of how intranuclear cTnI regulates *ATP2a2* expression by using ChIP-Seq and luciferase report assays. The data generated from our study have confirmed that cTnI does exist in nucleus of myocardial cells and the role of nuclear cTnI is involved in *Atp2a2* expression in the heart.

Materials and methods

Animals

Eight-week-old C57BL/6 male and female mice, five-week-old SD male rats were purchased from the Experimental Animal Center of Chongqing Medical University (Chongqing, China). All experimental procedures involving animals were approved by the Animal Care and Use Committee of Chongqing Medical University. Animal experiments were performed conforming to the NIH guidelines (Guide for the Care and Use of Laboratory Animals).[22] All animals were euthanized by overdose administration of pentobarbiturate (100−120 mg/kg).

Gene knock-out mice

Heterozygous $cTnI^{+/-}$ mutant mice were approved by Florida Atlantic University. $cTnI^{+/-}$ mice and littermate $cTnI^{+/+}$ mice were bred by hybridization of cTnI-knockout mice and wild type mice.

Animals models of heart failure (HF)

The SD rats were anesthetized by 30 mg/kg sodium pentobarbital. Atropine 0.05 mg/kg was administered subcutaneously. A core body temperature of approximately 37 °C was maintained during surgery by continuous monitoring with a rectal thermometer and automatic heating blanket. After mediastinotomy, the aorta was carefully identified.

A needle was placed on the aorta, on which a prolene ligation was placed. The needle was then carefully removed, and the transverse aortic constriction (TAC) was created, or for a sham operation (Sham). After the procedure, the wound was closed. One month after TAC, echocardiographic examination was performed under 1 ml/kg 10% chloral hydrate. Two-dimensional images and M-mode measurements were used to quantify left ventricular dimension and function. At least three sets of measures were obtained from three different cardiac cycles. It could be suggested from the result that heart failure model has successfully been established. The animals were sacrificed and the heart was removed for tissue sampling.

Clinical samples

Embryonic hearts samples were donated by two healthy couples without any cardiac diseases. They planned to take abortions because social factors. Subjects were obtained from The First Affiliated Hospital of Chongqing Medical University (Chongqing, China) in September 2016 and in November 2016. The local ethical committee of First Affiliated Hospital of Chongqing Medical University have approved the study. The procedures were performed in accordance with the Helsinki Declaration.

Neonatal mice ventricular myocytes (NMVMs) isolation and culture

As previously described, the primary myocardial cells were adopted from the ventricles of neonatal mice (in 3 days). Briefly, the cells were digested by 0.05% collagenase II, centrifuged by density gradient and collected to seed at a density of 1×10^6 cells/well in a 6-well plate. The cells were grown in F12/DMEM (1:1) containing 10% FBS, penicillin and streptomycin (50 U/mL), 5-fluorouracil (0.1 g/L), at 37 °C in humid air containing 5% CO_2. After 48 h of adhering, the culture medium was changing every day.

Western blotting

Fresh heart tissue was prepared and total protein was extracted by the Protein extraction kit (KGP2100, KeyGEN BioTECH, China). Cytoplasmic and nuclear protein were separated by Minute™ Cytoplasmic & Nuclear Extraction Kits (SC-003, Invent, USA) according to the manufacturer's instructions. Protein concentration was then quantitated with the Bradford protein quantitation assay (KGA803, KeyGEN BioTECH, China). 30 μg of total protein per lane was separated via SDS-PAGE gel and immunoblotted with primary antibodies against histone H3 (#4499, Cell Signaling Technology, USA), α-Tubulin (#2125, Cell Signaling Technology, USA), TnI (recognize both with mouse ssTnI and cTnI) (approved by Florida Atlantic University, as described in our previous studies[12,13,23]), GAPDH (Sino Biological, China), SERCA2a (#9580, Cell Signaling Technology, USA). Secondary antibodies were anti-rabbit (Sino Biological, China) or anti-mouse IgG HRP (Sino Biological, China), which were linked to the whole antibody. The immune-reactive protein bands were visualized and band intensity was analyzed and quantified by using Amersham Imager 600 system (GE Healthcare, USA).

Immunofluorescence

Cells cultured on slides were fixed with 4% paraformaldehyde (15 min at room temperature), and their membrane permeabilized at room temperature with 0.5% Triton X-100 in phosphate buffered saline (PBS) buffer for 5 min. After three washes with PBS, they were incubated in blocking buffer (PBS with 10% normal goat serum (Sigma, St Louis, MO) at room temperature for 1 h and were labeled at room temperature with primary and secondary antibodies for 2 h and 1 h, respectively. After cells were counterstained with DAPI (10236276001, Roche, Switzerland) mounted in Antifade Mounting Medium (KGF028, KeyGEN BioTECH, China). Immunofluorescence images were taken on a confocal microscopy (Olympus, IX81, Tokyo, Japan) with an Orca-R2 Hamamatsu CCD camera (Hamamatsu, Japan). Camera driver and image acquisition were controlled by a Meta Morph Imaging System (Olympus). Digital image files were transferred to Adobe Photoshop CS6 to assemble montages.

Weighted gene co-expression network analysis (WGCNA)

Expression datasets (GSE54681) were accessed from the GEO database, which represents the largest public repository for gene expression data. Data was first analyzed by using the original Series Matrix File data format provided in GEO. We respectively calculated correlation coefficients between every gene expression with TNNI3 in the dynamic process of heart failure. We used a correlation matrix with a cut-off of $r > 0.90$ for positive correlation and $r < -0.90$ for negative correlation. Through the "correlation analysis" of the other gene expression with *TNNI3* gene expression, the genes which have consistent expression with TNNI3 in time patterns (heart failure process) were obtained. We only analyzed genes positive which were related to TNNI3 by KEGG (Kyoto Encyclopedia of Genes and Genomes) pathways and GO (gene ontology) in the Database for Annotation, Visualization and Integrated Discovery (DAVID). Statistical analysis via hypergeometric test.

Total RNA extraction and quantitative real-time PCR analysis

The total RNA of all samples were extracted with the Tissue RNA kit (Bio Teke, China). cDNA was obtained by using the RevertAid First Strand cDNA Synthesis Kit (#K1622 Lot 00376308, Thermo Scientific, USA). The cDNA was amplified with SYBR® Green Master Mix kit (#A25741, Applied Biosystems, USA). Analyses of relative mRNA expression were

determined by using the $2^{-\Delta\Delta Ct}$ method, normalized to the expression of housekeeping gene. Primers for the genes were synthesized by Life Technologies Corporation (Shanghai, China). The primer (mouse) sequences of involved genes were designed as below:

TNNI3: 5′- AGGAGATGGAACGAGAGGCAGAAG -3' (forward primer)

5′- CGTGAAGCTGTCGGCATAAGTCC -3' (reverse primer)

Atp2a2: 5′- TTCTGCTTATCTTGGTAGCCAA -3' (forward primer)

5′- CTTTCTGTCCTGTCGATACACT -3' (reverse primer)

GAPDH:5′- AAGAAGGTGGTGAAGCAGGCATC -3' (forward primer)

5′- CGGCATCGAAGGTGGAAGAGTG -3' (reverse primer)

RNA interference (RNAi) assays

Synthetic siRNA oligonucleotides specific for *TNNI3* (5′-GGAGACTGGCGCAAGAATA-3′) was synthesized by Gene-Pharma (Shanghai, China). Stealth RNAi Negative Control Duplexes by GenePharma were used as negative controls. According to the manufacturer's instructions, NMVMs were transiently transfected with TNNI3 siRNA or negative control (NC) siRNA using Lipofectamine 2000 transfection reagent (Invitrogen, Carlsbad, CA, USA).

ATP assay

Myocardial tissue ATP content was determined by an Enhanced ATP Assay Kit (Beyotime, China) according to the manufacturer's instructions.

Cardiomyocyte Ca^{2+} imaging

NMVMs were planted in a 35 mm confocal dish and cultured for 48 h after transfection of siRNA. After three washes with PBS, cells were incubated in buffer [PBS with 2 μmol/L Fluo4-AM (Beyotime, China)] at room temperature for 30 min and then were washed with PBS three times again. Whole-cell fluorescent images of each cardiomyocyte incubated with PBS at 37 °C were recorded 600 times in 30 s by confocal microscopy. Calcium transient was shown by the changes of fluorescence intensity of cells.

Sarcoplasmic reticulum Ca^{2+} content assay

NMVMs were planted in 96-well black-walled, clear-bottom plates and cultured for 48 h after transfection of siRNA. After three washes with Tyrode's solution (no calcium) (Leagene Biotechnology, China), cells were incubated in buffer (Tyrode's solution with 2 μmol/L Fluo4-AM) at room temperature for 30 min and then were washed with Tyrode's solution three times again. Put the cell culture plate into Microplate System (Thermo Scientific, USA) and measure calcium responses at 37 °C for 100 ms at a time with 2s interval between successive readings at 525 nm. Setting the excitation of Fluo-4 to 488 nm and transfer a total volume of 100 μL of compound to the cell plate. 30 sec

after the reading start, Thapsigargin (MedChemexpres, USA) added with the final concentration of 5 μM we continuously monitored the fluorescence signal and calculate the $\Delta F/F_0$.

Chromatin immunoprecipitation sequencing (ChIP-Seq)

For chromatin immunoprecipitation, heart tissues were fixed with 1% formaldehyde for 10 min at room temperature with swirling. ChIP trials were conducted by use of SimpleChIP® Plus Enzymatic Chromatin IP Kit (#9005, Cell Signaling Technology, USA) according to the manufacturer's instructions. Samples were immunoprecipitated by using anti-cTnI, Histone H3 (D2B12) (#4620, Cell Signaling Technology, USA) and a nonspecific IgG control (#2729, Cell Signaling Technology, USA). Input groups that contain the protein-DNA complexes without antibodies were collected to show the total DNA in the samples.

ChIP-qPCR

By following the previous steps, purified DNA was subjected to quantitative PCR by using primers specific to the *Atp2a2* promoters. The primers (mouse) of involved DNA sequence were designed as below:

Site1: 5′- GGCTTCCCACATTCCTCTGC -3' (forward primer)

5′- GCCTGTGATCCCACGAACAG -3' (reverse primer)

Site2: 5′- CGGGCTCCGTATAGCCTCTT -3' (forward primer)

5′- TGGCTTCCAAATGATGGCTG -3' (reverse primer)

Site3: 5′- AAGCCAAGCCACCTAGCATAGC -3' (forward primer)

5′- ATCTCCATCGCACGCCAACAC -3' (reverse primer)

Site4: 5′- GGTGTTGGCGTGCGATGGAG -3' (forward primer)

5′- CCGTGCTCTGCATCCTAATGTCTC -3' (reverse primer)

Site5: 5′- GGCAAGCCAAGGACACCAGTG -3' (forward primer)

5′- GGATAGAGCGCGGAGTTCACG -3' (reverse primer)

Site6: 5′- CCGTGAACTCCGCGCTCTATC -3' (forward primer)

5′- CGTCCACGCTGTGCTCGATG -3' (reverse primer)

Cell culture and luciferase report

510bp promoter regions of mouse *Atp2a2*, which were detected by ChIP-Seq, were highly enriched with cTnI. In addition, these 510bp bases were amplified via PCR from genomic DNA of C57BL/6 mouse and were cloned into PGL3-basic (stored in our laboratory). After "A" were interchanged with "G", "T" were interchanged with "C", mutation vectors of pGL3- *Atp2a2* were constructed. The TNNI3 expression vector was prepared by cloning wild-type mouse *TNNI3* cDNA (661bp) into a pcDNA3.1 (−) vector. 293T cell lines (stored in our laboratory) were plated in 24-well plate reached to 90−95% confluent. PGL3-*Atp2a2*/Mut PGL3-Atp2a promoter fused firefly luciferase (300 ng/well), TK-renilla luciferase (2 ng/well) and pcDNA3.1(−)-*TNNI3*(300 ng/well) or pcDNA3.1(−)-null were transfected by Lipofectamine 2000 (NO.1769821, Invitrogen, USA). Luciferase activity was measured via a luciferase reporter assay (E1500, Promega, USA), with firefly luciferase activity normalized to renilla activity.
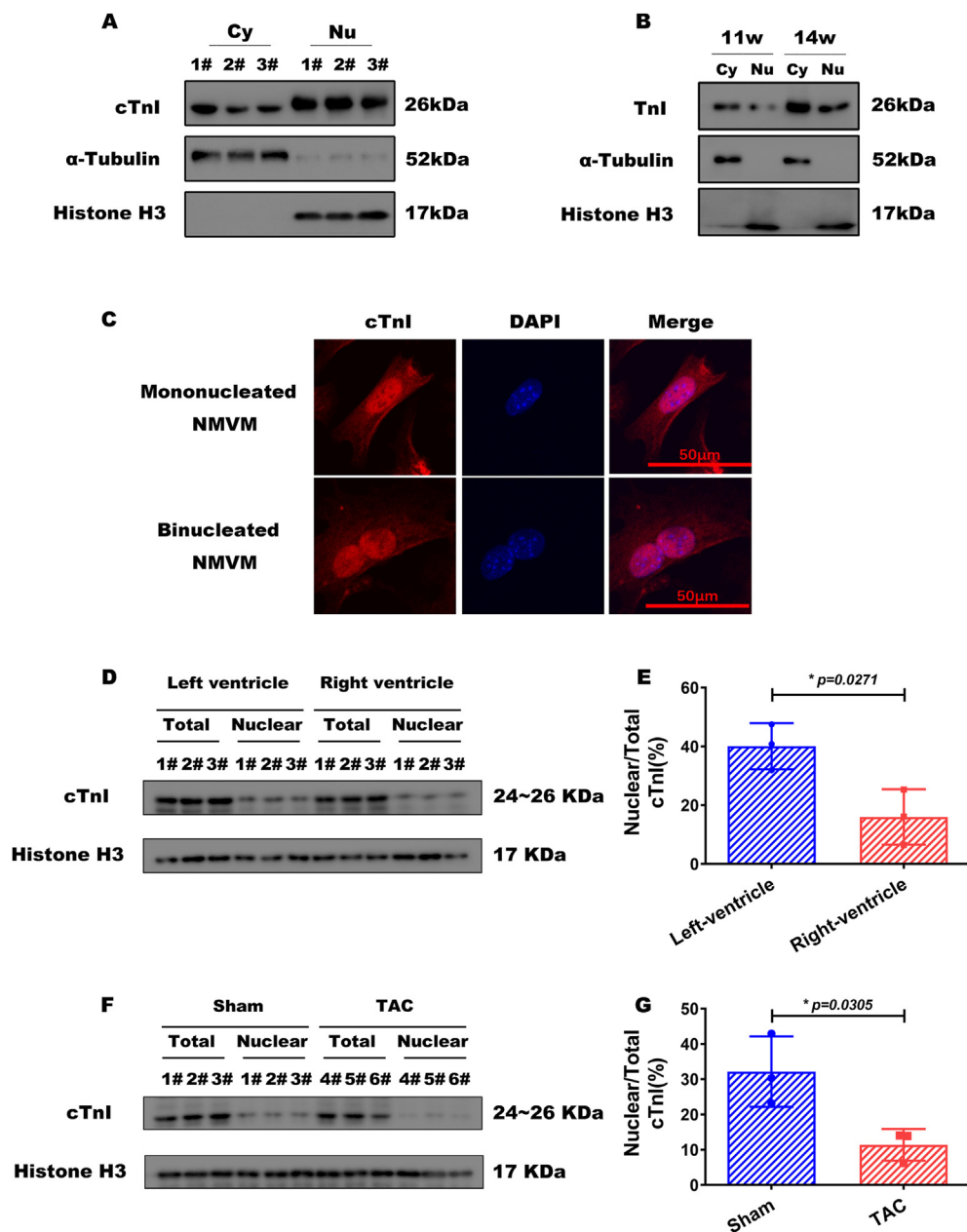
Figure 1 Detecting of intranuclear cTnI in physiological and pathological conditions. **(A)** Immunoblotting of cTnI in nuclear (Nu) and cytoplasm (Cy) lysates of adult mice cardiomyocytes. **(B)** Immunoblotting of cTnI in nuclear (Nu) and cytoplasm (Cy) lysates of human fetal hearts (11- and 14-week's embryos). **(C)** cTnI was examined in neonatal mice ventricular myocytes through fluorescence microscope. Scale bars show 50 μm. **(D—E)** Intranuclear cTnI detection both in left and right ventricles of wild type adult mouse hearts. Western blot analysis were expressed as Mean ± SEM derived from $n = 3$ independent experiments analyzed by Mann—Whitney test. *$P < 0.05$ as compared with controls. **(F—G)** Intranuclear cTnI detection in left ventricles of mice with heart failure and wild type mice. The results are expressed as mean ± SEM from $n = 3$ separate experiments. *$P < 0.05$ as compared with controls analyzed by Mann—Whitney test.

Protein immunoprecipitation

Protein immunoprecipitation was performed as previous described.[18] In brief, immunoprecipitation protein lysis buffer was added with protease inhibitors (4693116001, Roche, USA) and phosphatase inhibitors (4906837001, Roche, USA). Mouse heart tissue were lysed using protein lysis buffer and were incubated with the primary antibodies

(1—2 μg) (cTnI as previous described, YY1 (#63227, Cell Signaling Technology, USA) and IgG control antibody (#SC69786, Santacruz)) for 4 h at 4 °C. The incubation tubes were added with Pierce Protein A/G Magnetic Beads (88802, Thermo Scientific, USA) to incubate for 1 h and washed four times with magnetic separation. Add 100 μL of 1 × SDS-PAGE to the tube and heat the samples at 96—100 °C for 10 min. Magnetically separate the beads and

save the supernatant containing target antigen. Protein solution (10 uL) was then used in Western blotting analysis (described above).

Statistical analysis

All data were expressed as Means $\pm$ SEM. Comparisons between groups were made by using unpaired Mann Whitney test. For comparison of more than two groups with comparable variances, one-way ANOVA was carried out. $P < 0.05$ was considered to be significant. All experiments were repeated at least three times with triplicate samples, and representative data were shown.
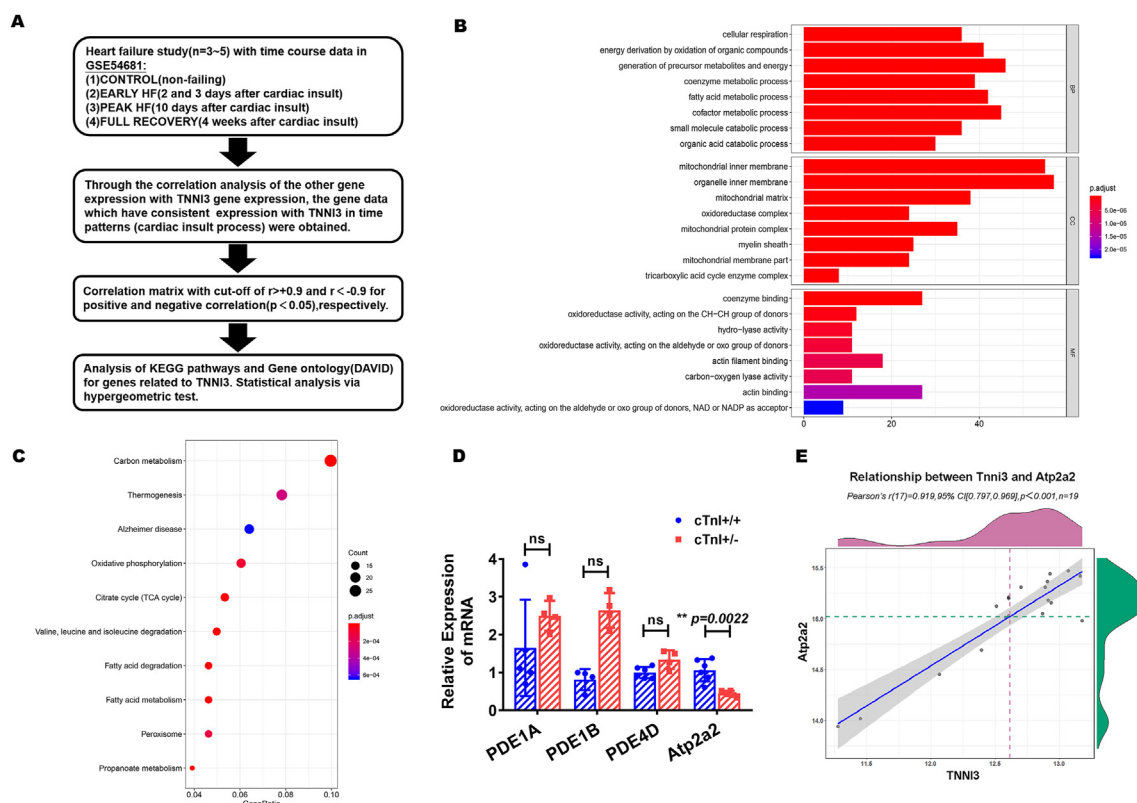
Results

Detecting of intranuclear cTnI in physiological and pathological conditions

To explore the nuclear translocation of cTnI, we extracted and separated heart tissue into Nu and Cy. cTnI in cytoplasm or in the nucleus were tested by Western blotting. α-

Tubulin was chosen as cytoplasmic protein marker, and Histone H3 was selected as nuclear protein marker by reference 18. A certain amount of TnI expressed in the nucleus in adult mice and human fetal hearts (Fig. 1A, B). There were at least two developmentally regulated TnI isoforms in the heart: the slow skeletal TnI (ssTnI) that was expressed first and predominates throughout embryonic and fetal development and the cardiac TnI (cTnI) that was predominately expressed in adult hearts. We only obtained 2 human fetal hearts (11-week and 14-week). Moreover, the anti-TnI monoclonal antibody we used in this study could recognize both cTnI and ssTnI. Therefore, in embryonic day of 11-week and 14-week, the TnI that we detected in the nuclear might contain both ssTnI and cTnI. Indirect immunofluorescence tests showed that cTnI was expressed in the nucleus of mice cardiomyocytes with confocal laser scanning microscope (Fig. 1C).

To determine the effect of the phenomenon in physiology, the ratio of nuclear/total-cTnI in rats' right ventricular heart tissues was contrasted with that in left ventricular heart tissues. The ratio in right ventricular heart tissues was significantly lower than that in left ($n = 3$, $P = 0.0271$) (Fig. 1D, E). To further investigate the role of

Figure 2 Weighted gene co-expression network analysis (WGCNA) of cTnI and verification results in a knock-out mice model. **(A)** The flow charts of WGCNA of *TNNI3*. **(B, C)** Genes positive related to *TNNI3* were analyzed by KEGG (Kyoto Encyclopedia of Genes and Genomes) pathways and GO (Gene ontology) in the Database for Annotation, Visualization and Integrated Discovery (DAVID). **(D)** RT-qPCR of candidate genes of PDE1A, PDE1B, PDE4D and *ATP2a2* in *TNNI3* knockout mice. The results are expressed as mean $\pm$ SEM from $n = 4-6$ separate experiments. ** means $P < 0.01$ as compared with $cTnI^{+/+}$ group analyzed by Mann−Whitney test. **(E)** Correlation coefficient between *ATP2a2* expression with *TNNI3* in the dynamic process of heart failure was calculated. (Pearson's R $= 0.919$ 95%CI [0.797, 0.969] $P < 0.001$, $n = 19$).

the subcellular distribution of cTnI particularly in pathological conditions, we constructed a rat model of left ventricular heart failure with reduced ejection fraction (EF) and increased left ventricular end-diastolic pressure (LVEDP) by transverse aortic coarctation (TAC) (Fig. S1 and Table S1). The ratio of nuclear/total-cTnI in TAC groups was remarkably decreased compared with that in sham group ($n = 3$, $P = 0.0305$) (Fig. 1F, G).

Weighted gene co-expression network analysis (WGCNA) of cTnI in a heart failure model

We identified a HF study (GSE54681) in GEO database and used WGCNA to calculate the correlation coefficient between candidate genes and TNNI3 in HF developing process (Table S2). A flowchart of the experimental design and analyze process is shown in Figure 2A. It came to a surprise that cTnI performed a closely related pattern with some energy metabolism processes and calcium homeostasis regulation, not just a binding protein with actin filaments (Fig. 2B, C). We predicted several suspicious downstream genes of cTnI, by calculating the correlation coefficient, and we confirmed *Atp2a2*, *PDE1A*, *PDE1B* and *PDE4D* as the candidate genes ($R > 0.9$). In our following cell experiments, the data indicated that only *Atp2a2*

expression could be regulated significantly by *TNNI3* ($n = 6$, $P = 0.0022$) (Fig. 2D). *Atp2a2* performed a strong association expression pattern with *TNNI3* ($r = 0.919$) (Fig. 2E).
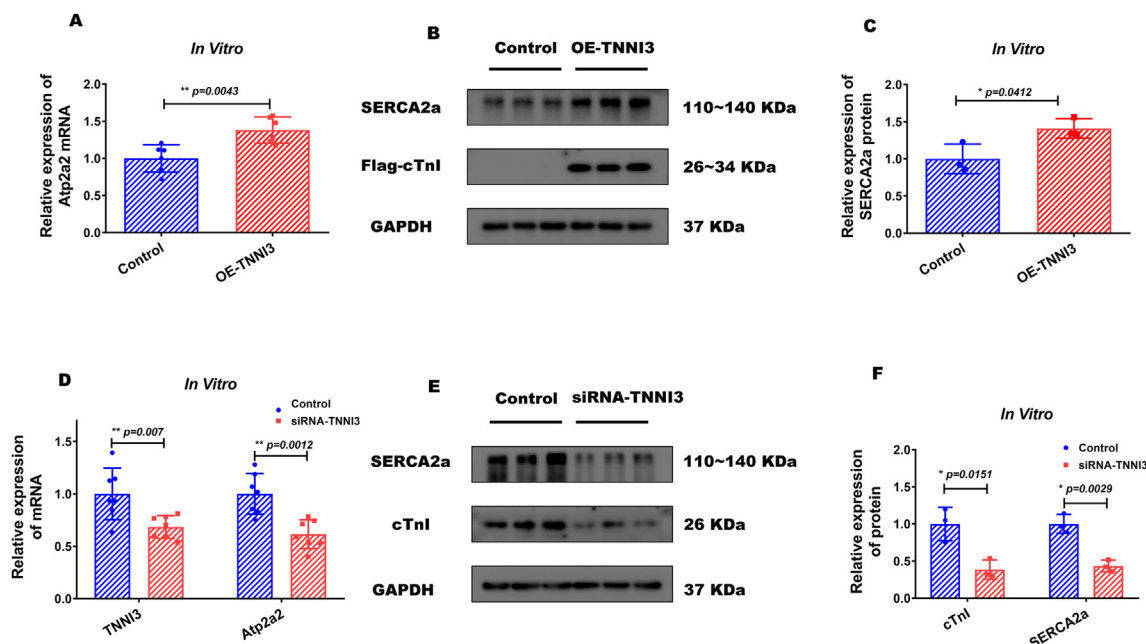
ATP2a2/SERCA2a expression levels after cTnI gain and loss *in vivo*

To study the regulatory effects of cTnI *in vivo*, we firstly constructed over-expressed TNNI3 (OE-TNNI3) mice model by tail vein injecting TNNI3 recombinant adenoviruses into 8 weeks old C57BL/6 mice. mRNA levels of *ATP2a2* in the heart tissues of the OE-TNNI3 group were significantly up-regulated compared with that in control group ($n = 8{-}10$, $P < 0.0001$) (Fig. 3A). Similarly, protein levels of SERCA2a (encodes by *Atp2a2*) of OE-TNNI3 group were higher than that in control group ($n = 3$, $P = 0.0428$) (Fig. 3B, C).

To better examine regulatory effect of cTnI on *Atp2a2 in vivo*, we used a *cTnI* knocked out mouse model.[11] As shown in Figure 3D, *Atp2a2* mRNA levels in $cTnI^{+/-}$ mice were decreased significantly compared with controls ($n = 10{-}11$, $P < 0.0001$). Similarly, in cTnI loss mice, SERCA2a protein levels were decreased as well ($n = 3$, $P = 0.0011$). Interestingly, content of intranuclear cTnI in
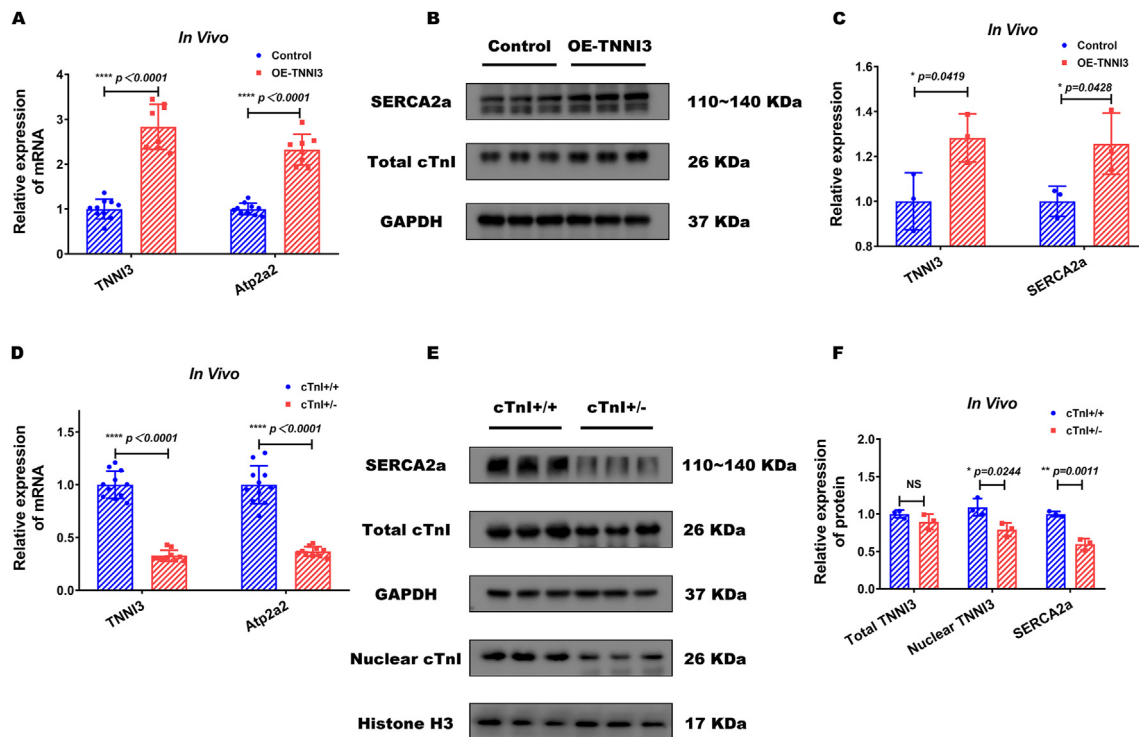
Figure 3 *ATP2a2*/SERCA2a expression levels after cTnI gain and loss *in vivo*. **(A)** mRNA levels of *ATP2a2* in cTnI over-expression mice. The results are expressed as mean $\pm$ SE from $n = 8{-}10$ separate experiments. *** means $P < 0.001$ as compared with controls analyzed by Mann−Whitney test. **(B, C)** Immunoblotting of *cTnI* and SERCA2a in cTnI over-expression mice. Western blot analysis were expressed as Mean $\pm$ SEM derived from $n = 3$ independent experiments analyzed by Mann−Whitney test. *$P < 0.05$ as compared with controls. **(D)** mRNA levels of *ATP2a2* in *cTnI* knockout mice($cTnI^{+/-}$). The results are expressed as mean $\pm$ SE from $n = 11$ separate experiments. *** means $P < 0.001$ as compared with controls analyzed by Mann−Whitney test. **(E, F)** Immunoblotting of cTnI and SERCA2a in $cTnI^{+/-}$ mice, and immunoblotting of cTnI in nuclear (Nu) lysates of cTnI $\pm$ mice. Western blot analysis were expressed as Mean $\pm$ SEM derived from $n = 3$ independent experiments analyzed by Mann−Whitney test. *$P < 0.05$, **$P < 0.01$ as compared with controls.

Figure 4 *ATP2a2*/SERCA2a expression levels after cTnI gain and loss *in vitro*. **(A)** mRNA levels of *ATP2a2* in over-expression *TNNI3* neonatal mice ventricular myocytes. The results are expressed as mean ± SE from $n = 6$ separate experiments. ** means $P < 0.01$ as compared with controls analyzed by Mann−Whitney test. **(B, C)** Immunoblotting of Flag-cTnI and SERCA2a in over-expression *TNNI3* NMVMs. Western blot analysis were expressed as Mean ± SEM derived from $n = 3$ independent experiments analyzed by Mann−Whitney test. *$P < 0.05$ as compared with controls. **(D)** mRNA levels of *ATP2a2* in NMVMs of *TNNI3* knock-down by siRNA(-siRNA-*TNNI3*). The results are expressed as mean ± SE from $n = 7$ separate experiments. ** means $P < 0.01$ as compared with controls analyzed by Mann−Whitney test. **(E, F)** Immunoblotting of cTnI and SERCA2a in siRNA-*TNNI3* NMVMs. Western blot analysis were expressed as Mean ± SEM derived from $n = 3$ independent experiments analyzed by Mann−Whitney test. *$P < 0.05$ as compared with controls.

$cTnI^{+/-}$ mice was significantly lower than that in littermate $cTnI^{+/+}$ mice ($n = 3$, and $P = 0.0011$) (Fig. 3E, F).

ATP2a2/SERCA2a expression levels after cTnI gain and loss *in vitro*

Neonatal mice cardiomyocytes were cultured *in vitro*. Certainly, mRNA levels of *ATP2a2* in cells transfected with TNNI3/cTnI recombinant adenoviruses were increased compared to controls ($n = 6$, $P = 0.0043$) (Fig. 4A). Protein levels of SERCA2a in OE group were higher than those in controls ($n = 3$, $P = 0.0412$) (Fig. 4B, C).

mRNA levels of *ATP2a2* in cells with TNNI3-siRNA were much lower than those in NC-siRNA group ($n = 7$, $P = 0.0012$) (Fig. 4D). Protein levels of SERCA2a significantly declined in cells that transfected with TNNI3-siRNA ($n = 3$, $P = 0.0029$) (Fig. 4E, F).

Function evaluation after cTnI loss in cardiomyocytes

cTnI knockout mouse was found with shortened sarcomeres and elevated resting tension measured under relaxing conditions, and had a reduced myofilament Ca^{2+} sensitivity under activating conditions.[19] SERCA2a is closely related

with ATP utilization and Ca^{2+} transients. After TNNI3 being silence by siRNAs, beat frequency (BF) of cardiomyocytes declined both after 24 h and 48 h culture (Fig. 5A). Furthermore, ATP content in cells accumulated ($n = 6$, $P = 0.0022$) (Fig. 5B). Compared with the control group, intracellular calcium transient frequency in TNNI3-siRNA group was significantly reduced (Fig. 5C−E and supplementary movie).

Binding affinity of cTnI on promoter of *ATP2a2*

Binding levels of cTnI with *ATP2a2*'s promoter region was detected by ChIP-seq technology in the heart tissue of c57 mice, specific binding DNA sequences of cTnI were enriched in *ATP2a2* promoter $-239 \sim -889$ region (Fig. 6A). The specific binding sequence motif of cTnI was analyzed by software as "CCAT", which has been reported to be required for *YY1* binding to the promoter region of *YY1*-related genes (Fig. 6B−D). The binding levels of each segment in the promoter region of *ATP2a2* were verified by ChIP-qPCR (Fig. 6E, F). The interactions between *YY1* and cTnI were detected with immunoprecipitation (Fig. 6G). In 293A cells, pcDNA3.1 plasmid/TNNI3 over-expression plasmid and *ATP2a2* promoter luciferase reporter gene plasmid were co-transfected. Compared with control group, the luciferase
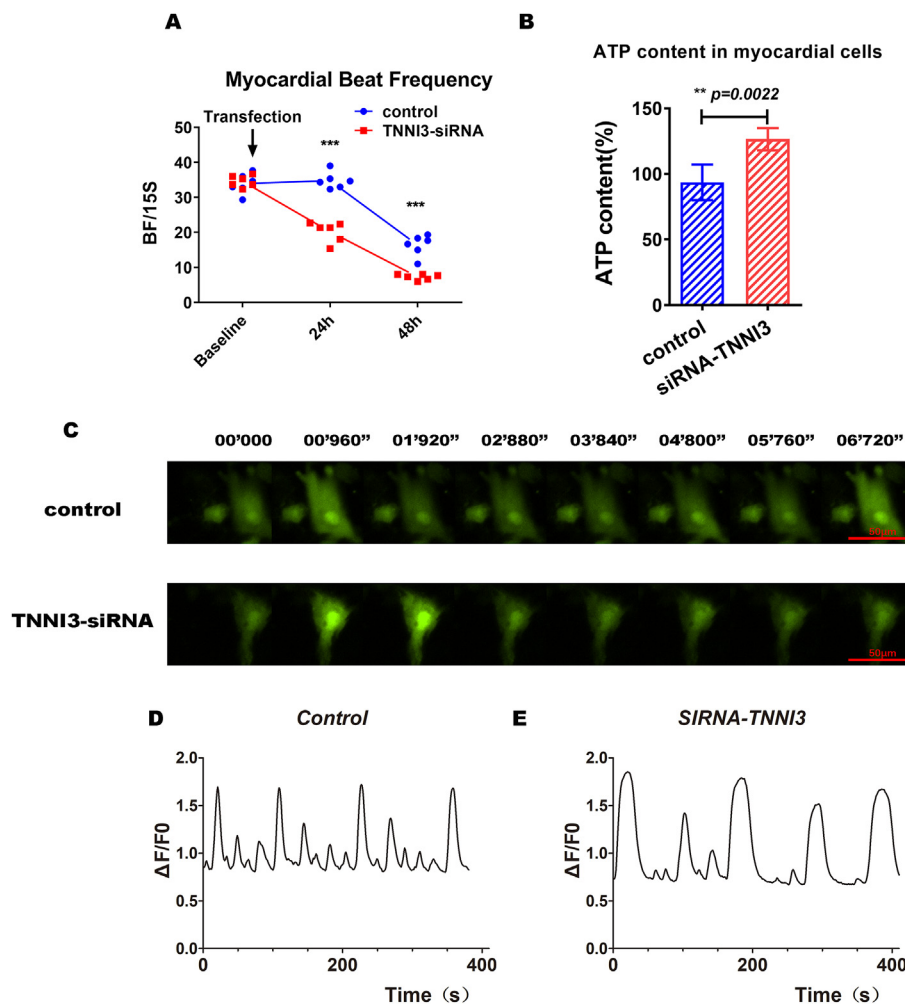
Figure 5 Calcium dyshomeostasis after cTnI loss in cardiomyocytes. **(A)** Beat frequencies of cardiomyocytes after transfecting siRNA-*TNNI3*. *** means $P < 0.001$ as compared with controls. **(B)** Total ATP contents in cardiomyocytes of siRNA-*TNNI3* groups compared with controls. ** means $P < 0.01$ as compared with controls. **(C)** NMVMs loaded fluo4-AM were detected by laser confocal microscopy. Scale bars show 50 μm. **(D, E)** Intracellular calcium transient frequencies of siRNA-*TNNI3* and control groups.

activities significantly increased in cells transfected with pcDNA3.1-TNNI3 plasmid ($n = 6$, $P < 0.0001$) (Fig. 6H).

Discussion

Recent data have identified potential TNNT2-interacting nuclear proteins, such as KDM1A and KDM5A.[21] More importantly, increased nuclear localization of mutated TNNT2 might enhance the interaction of TNNT2 with these key epigenetic.[21] Zhang et al[19,24] found that TnT3 shuttles to the nucleus, where it appears to perform nonclassical transcription regulatory functions. In our study, another thin filament component, cTnI was explored as an intranuclear protein. We found that it could regulate *Atp2a2* transcription and then impact myocardial systolic/diastolic abilities.

cTnI is known for its association with cardiac diastolic function. *cTnI* knockout mice died of acute diastolic heart failure on Day 18, demonstrating that TnI is required for normal cardiac function and survival.[11] Recently, cTnI is known as a serum biomarker for evaluating myocardial

tissue damages,[25] and as a subunit of the thin filament-associated troponin-tropomyosin complex involved in calcium regulation.[26,27] However, it's worthy noting that several studies have suggested that TnI could be found in the nucleus.[5,12,15] More importantly, our data have firstly demonstrated that TnI is located in nuclear of fetal human hearts. Unfortunately, we did not measure subtype of TnI, ssTnI or cTnI,[11] in human fetal hearts. It is interesting to find that levels of cTnI nucleoprotein in left ventricle are higher than that in right ventricle. Moreover, intranuclear cTnI proteins are declined in left ventricles of heart failure than that in controls. Systolic function of the left ventricle is usually stronger than that of right ventricle, and heart functions of a failure heart are significantly decreased. Therefore, we speculate that contents of intranuclear of cTnI in cardiomyocytes may associate with heart functions. More importantly, cTnI was localized in the nucleus of hearts. This part of cTnI could hardly be ignored. Although mechanisms of cTnI transportation to the nucleus are unknown, functional analysis of intranuclear cTnI is of great value.
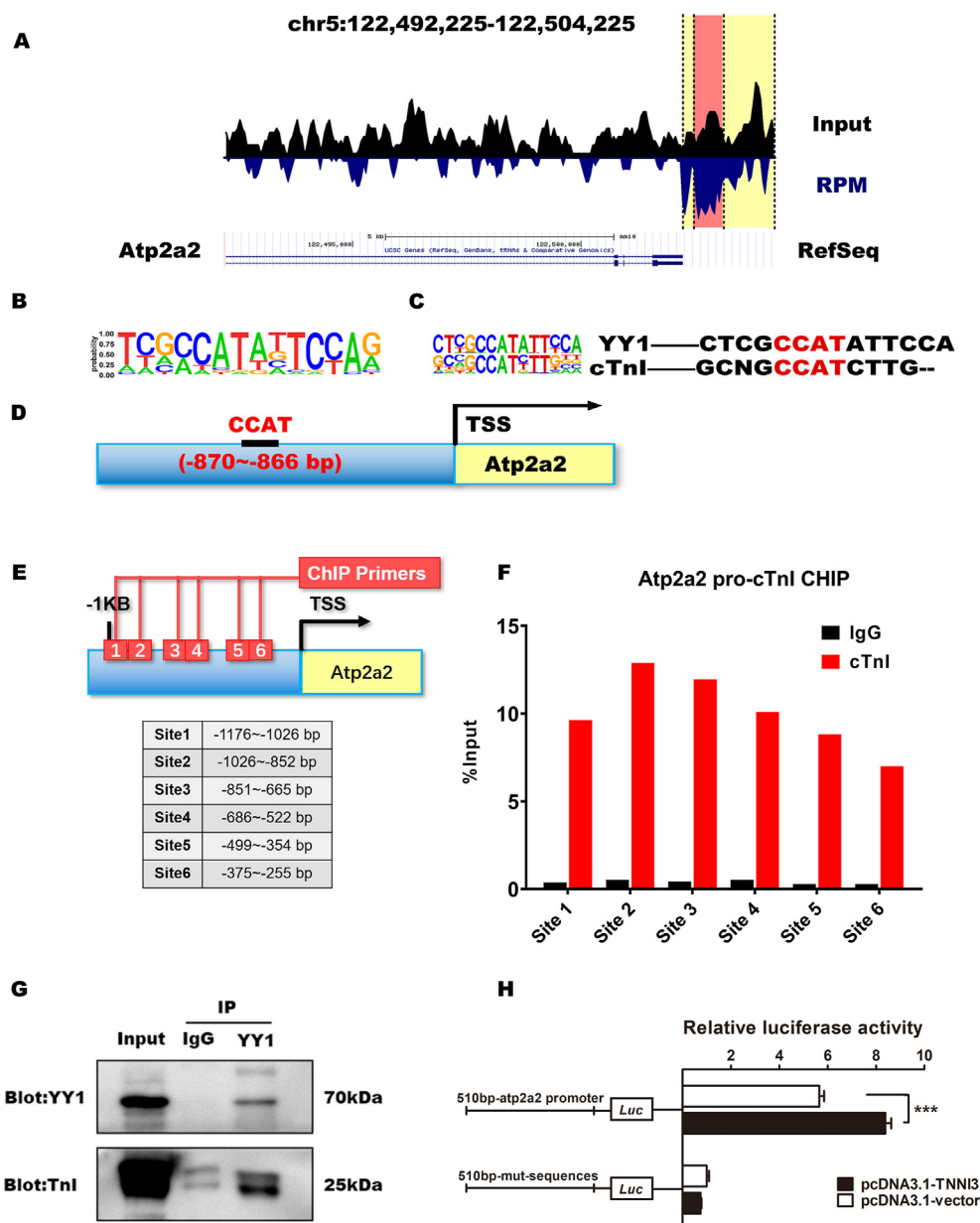
Figure 6 Binding affinity and binding regions of cTnI with promoter of *ATP2a2*. **(A)** Specific binding DNA sequences of cTnI were enriched in *ATP2a2* promoter −239∼−889 region. **(B, C)** Binding sequence motif of cTnI was analyzed by software as "CCAT", which has been reported to be required for *YY1* binding to the promoter region of *YY1*-related genes. **(D)** "CCAT" sequence was in the promoter region of *ATP2a2*. **(E)** The promoter region of *ATP2a2* were divided into 6 segments. **(F)** Binding abilities of cTnI with each segment were verified by CHIP-qPCR. **(G)** Immunoblotting (IB) of cTnI in the lysates (input) or immunoprecipitates (IP; IgG or anti-*YY1*) of NMVMs. **(H)** In 293A cells, relative luciferase activity was shown after pcDNA3.1 plasmid/*TNNI3* over-expression plasmid and *ATP2a2* promoter luciferase reporter gene plasmid co-transfection. *** means $P < 0.001$ as compared with controls analyzed by Mann−Whitney test.

We analyzed potential pathways and genes that show strong correlations with TNNI3 through bioinformatics analysis. Surprisingly, Genes like *PDE1a*, *PDE2a*, *PDE4d*, *Atp2a1*, *Atp2a2* and *Atp2a3* showed strong correlations with cTnI expression. We detected mRNA levels of these genes after TNNI3 knock down in cell models, only *Atp2a2* showed a linear expression pattern with TNNI3. SERCA2a was also down regulated by cTnI loss both *in vivo* and *in vitro*. Gain of cTnI induces increases of *Atp2a2* in mRNA and protein levels, both *in vitro* and *in vivo*. These data indicate a strong correlation between cTnI and *Atp2a2*. In Figure 3F, nuclear cTnI of *cTnI*$^{+/-}$ mice were decreased, accompanied with a significant decrease of Serca2a.

cTnI loss or mutations could induce heart failures, heart aging or CMs,[8,11,12,28] some pathological changes, such as energy metabolism disorders and calcium

regulatory imbalance in these diseases cannot be well explained if cTnI is just a cytoplasmic protein. Furthermore, it has been demonstrated that SERCA2a decrease significantly in heart failure and aging hearts, both in human and mice.[29–31] Our data strongly suggested that cTnI might regulate *Atp2a2* expression as a nuclear protein. Therefore, in current study, we identified genome-wide sequence motifs targeted by nuclear cTnI in heart tissues by using ChIP-Seq analysis. Moreover, the motif identified the sequence CCAT, which is enriched in promoter of *Atp2a2*, also required for *YY1* binding to the promoter area of *YY1* related genes.[32,33] *YY1* has been shown for its regulatory role in controlling *Atp2a2* transcription activity through binding with CCAT motif. Also, binding abilities of cTnI and *YY1* was confirmed. So, luciferase report assay was used for detecting whether intranuclear cTnI could activate *Atp2a2*'s transcription. Interestingly, cTnI promoted transcriptional activities of *Atp2a2*. These data indicate that cTnI might control *Atp2a2* through binding with *YY1*.

Our data demonstrate that cTnI could regulate *Atp2a2*. SERCA2a enzyme catalyzed the hydrolysis of ATP coupled with the translocation of calcium from the cytosol to the sarcoplasmic reticulum lumen, and was involved in calcium sequestration associated with muscular excitation and contraction.[34] SERCA2a showed regulation roles both in energy metabolism and calcium regulatory.[35] In this study, we treated *TNNI3*-siRNA myocardial cells with TG, a non-competitive inhibitor of SERCA. The calcium concentration in SR of *TNNI3*-siRNA myocardial cells were found to decrease remarkably. In addition, our results suggested that cTnI loss induced an accumulation of ATP and numerous cytoplasmic vacuoles (data not shown), which is known as a senescence marker.[36] cTnI is known for its close relationship with cardiac function, so our data showed that the down regulated SERCA2a expression induced by cTnI loss cause the cardiac dysfunction, which supplemented mechanisms of cTnI loss affect heart dysfunction.

Conclusions

In present study, our data showed the nuclear translocation of cTnI, and intranuclear cTnI might regulate *Apt2a2* transcription level through binding with a classic transcription factor *YY1*, and then affect cardiomyocytes contraction and relaxation. These results indicate a novel role of cTnI, and might provide new aspects for investigations in heart development and cardiovascular diseases.

Ethics approval and consent to participate

This study was approved by the Institutional Review Board of Children's Hospital of Chongqing Medical University and the ethical committee of First Affiliated Hospital of Chongqing Medical University. The procedures were performed in accordance with the Helsinki Declaration.

Author contributions

JT, BP, and XL conception and design of research; QL, BP, GL and WAZ performed the experiment; LJL, TWL and HBB analyzed data; QL, RML and XPH interpreted results of experiments; QL and BP prepared figures; QL XPH and BP drafted manuscript. All authors read and approved the final manuscript.

Conflict of interests

The authors have no conflicts of interest to declare.

Funding

Acknowledgements

Availability of data and materials

All relevant data and materials are stored at Children's Hospital of Chongqing Medical University and can be obtained from the first author and corresponding author.

Appendix A. Supplementary data

Supplementary data to this article can be found online at https://doi.org/10.1016/j.gendis.2021.04.007.

References

1. Tobacman LS. Thin filament-mediated regulation of cardiac contraction. *Annu Rev Physiol*. 1996;58:447–481.
2. Reichlin T, Hochholzer W, Bassetti S, et al. Early diagnosis of myocardial infarction with sensitive cardiac troponin assays. *N Engl J Med*. 2009;361(9):858–867.
3. Pouleur H. Diastolic dysfunction and myocardial energetics. *Eur Heart J*. 1990;11(Suppl C):30–34.
4. Murphy RT, Mogensen J, Shaw A, Kubo T, Hughes S, McKenna WJ. Novel mutation in cardiac troponin I in recessive idiopathic dilated cardiomyopathy. *Lancet*. 2004;363(9406): 371–372.
5. Kimura A, Harada H, Park JE, et al. Mutations in the cardiac troponin I gene associated with hypertrophic cardiomyopathy. *Nat Genet*. 1997;16(4):379–382.
6. Li Y, Charles PY, Nan C, et al. Correcting diastolic dysfunction by Ca2+ desensitizing troponin in a transgenic mouse model of restrictive cardiomyopathy. *J Mol Cell Cardiol*. 2010;49(3): 402–411.
7. Morimoto S. Sarcomeric proteins and inherited cardiomyopathies. *Cardiovasc Res*. 2008;77(4):659–666.

8. Liu X, Zhang L, Pacciulli D, et al. Restrictive cardiomyopathy caused by troponin mutations: application of disease animal models in translational studies. *Front Physiol*. 2016;7:629.

9. Parvatiyar MS, Pinto JR, Dweck D, Potter JD. Cardiac troponin mutations and restrictive cardiomyopathy. *J Biomed Biotechnol*. 2010;2010:350706.

10. Li Y, Zhang L, Jean-Charles PY, et al. Dose-dependent diastolic dysfunction and early death in a mouse model with cardiac troponin mutations. *J Mol Cell Cardiol*. 2013;62:227–236.

11. Huang X, Pi Y, Lee KJ, et al. Cardiac troponin I gene knockout: a mouse model of myocardial troponin I deficiency. *Circ Res*. 1999;84(1):1–8.

12. Pan B, Xu ZW, Xu Y, et al. Diastolic dysfunction and cardiac troponin I decrease in aging hearts. *Arch Biochem Biophys*. 2016;603:20–28.

13. Pan B, Quan J, Liu L, et al. Epigallocatechin gallate reverses cTnI-low expression-induced age-related heart diastolic dysfunction through histone acetylation modification. *J Cell Mol Med*. 2017;21(10):2481–2490.

14. Ritterhoff J, Tian R. Metabolism in cardiomyopathy: every substrate matters. *Cardiovasc Res*. 2017;113(4):411–421.

15. Sahota VK, Grau BF, Mansilla A, Ferrús A. Troponin I and Tropomyosin regulate chromosomal stability and cell polarity. *J Cell Sci*. 2009;122(Pt 15):2623–2631.

16. Asumda FZ, Chase PB. Nuclear cardiac troponin and tropomyosin are expressed early in cardiac differentiation of rat mesenchymal stem cells. *Differentiation*. 2012;83(3):106–115.

17. Kehat I, Kenyagin-Karsenti D, Snir M, et al. Human embryonic stem cells can differentiate into myocytes with structural and functional properties of cardiomyocytes. *J Clin Invest*. 2001;108(3):407–414.

18. Zhao W, Wu X, Wang Z, et al. Epigenetic regulation of phosphodiesterase 4d in restrictive cardiomyopathy mice with cTnI mutations. *Sci China Life Sci*. 2020;63(4):563–570.

19. Zhang T, Birbrair A, Wang ZM, Taylor J, Messi ML, Delbono O. Troponin T nuclear localization and its role in aging skeletal muscle. *Age (Dordr)*. 2013;35(2):353–370.

20. Nunez Lopez YO, Messi ML, Pratley RE, Zhang T, Delbono O. Troponin T3 associates with DNA consensus sequence that overlaps with p53 binding motifs. *Exp Gerontol*. 2018;108:35–40.

21. Wu H, Lee J, Vincent LG, et al. Epigenetic regulation of phosphodiesterases 2A and 3A underlies compromised beta-adrenergic signaling in an iPSC model of dilated cardiomyopathy. *Cell Stem Cell*. 2015;17(1):89–100.

22. National Research Council (US). Committee for the Update of the Guide for the Care and Use of Laboratory Animals. Guide for the Care and Use of Laboratory Animals. 8th ed. Washington (DC): National Academies Press (US); 2011.

23. Liu J, Du J, Zhang C, Walker JW, Huang X. Progressive troponin I loss impairs cardiac relaxation and causes heart failure in mice. *Am J Physiol Heart Circ Physiol*. 2007;293(2):H1273–H1281.

24. Zhang T, Birbrair A, Delbono O. Nonmyofilament-associated troponin T3 nuclear and nucleolar localization sequence and leucine zipper domain mediate muscle cell apoptosis. *Cytoskeleton (Hoboken)*. 2013;70(3):134–147.

25. Reiter M, Twerenbold R, Reichlin T, et al. Early diagnosis of acute myocardial infarction in patients with pre-existing coronary artery disease using more sensitive cardiac troponin assays. *Eur Heart J*. 2012;33(8):988–997.

26. Gunther LK, Feng HZ, Wei H, et al. Effect of N-terminal extension of cardiac troponin I on the Ca(2+) regulation of ATP binding and ADP dissociation of myosin II in native cardiac myofibrils. *Biochemistry*. 2016;55(12):1887–1897.

27. Wei H, Jin JP. NH2-terminal truncations of cardiac troponin I and cardiac troponin T produce distinct effects on contractility and calcium homeostasis in adult cardiomyocytes. *Am J Physiol Cell Physiol*. 2015;308(5):C397–C404.

28. Welsh TM, Kukes GD, Sandweiss LM. Differences of creatine kinase MB and cardiac troponin I concentrations in normal and diseased human myocardium. *Ann Clin Lab Sci*. 2002;32(1):44–49.

29. Schmidt U, del Monte F, Miyamoto MI, et al. Restoration of diastolic function in senescent rat hearts through adenoviral gene transfer of sarcoplasmic reticulum Ca(2+)-ATPase. *Circulation*. 2000;101(7):790–796.

30. Miyamoto MI, del Monte F, Schmidt U, et al. Adenoviral gene transfer of SERCA2a improves left-ventricular function in aortic-banded rats in transition to heart failure. *Proc Natl Acad Sci U S A*. 2000;97(2):793–798.

31. Tarazón E, Ortega A, Gil-Cayuela C, et al. SERCA2a: a potential non-invasive biomarker of cardiac allograft rejection. *J Heart Lung Transplant*. 2017;36(12):1322–1328.

32. Nan C, Huang X. Transcription factor Yin Yang 1 represses fetal troponin I gene expression in neonatal myocardial cells. *Biochem Biophys Res Commun*. 2009;378(1):62–67.

33. Hyde-DeRuyscher RP, Jennings E, Shenk T. DNA binding sites for the transcriptional activator/repressor YY1. *Nucleic Acids Res*. 1995;23(21):4457–4465.

34. Chen X, Zhang X, Gross S, Houser SR, Soboloff J. Acetylation of SERCA2a, another target for heart failure treatment? *Circ Res*. 2019;124(9):1285–1287.

35. Park WJ, Oh JG. SERCA2a: a prime target for modulation of cardiac contractility during heart failure. *BMB Rep*. 2013;46(5):237–243.

36. Shubin AV, Demidyuk IV, Komissarov AA, Rafieva LM, Kostrov SV. Cytoplasmic vacuolization in cell death and survival. *Oncotarget*. 2016;7(34):55863–55889.